RSC Advances

The homogeneous Au-Pd NPs with small size have been prepared through a facile *in-situ* reduction method. The optimal $AuPd_{1.0}/SiO_2$ catalyst could complete the conversion of chlorobenzene within 2 h at 25 ^oC. The significantly improved catalytic performance of the bimetallic catalyst can be ascribed to the high dispersion and modified electronic properties of Pd.
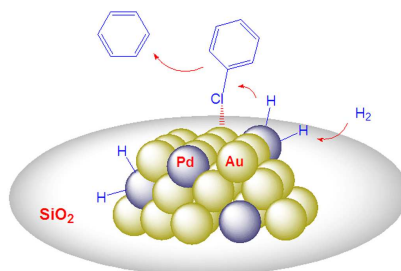
PAPER

In-situ synthesis of Au-Pd bimetallic nanoparticles on amine-functionalized SiO₂ for the aqueous-phase hydrodechlorination of chlorobenzene

Xinkui Wang,*[ab] Qinggang Liu,[b] Zihui Xiao,[b] Xiao Chen,[b] Chuan Shi,[b] Shengyang Tao,[b] Yanqiang Huang,[c] and Changhai Liang[b]

Highly dispersed Au-Pd nanoparticles (NPs) with an average size of ~ 3.0 nm were synthesized by *in-situ* reduction of HAuCl₄ and PdCl₂ on an amine-functionalized SiO₂ support. The structural and electronic properties of the Au-Pd NPs were investigated systematically using STEM-EDX, XRD, UV-vis and XPS spectroscopy. It is demonstrated that the composition of the Au-Pd NPs can be tuned by varying the ratio of Au- to Pd-containing salt in solution. In the aqueous-phase hydrodechlorination of chlorobenzene, the Au-Pd NPs showed a much higher activity and chlorine resistance than the monometallic Au and Pd counterparts. The effects of base and solvent on the activity over the supported Au-Pd NPs were also investigated.

1. Introduction

Aryl chlorides have been widely used as solvents, odorizers, insect repellents, fungicides, and intermediates in the synthesis of organic chemicals.[1] Unfortunately, these aryl chlorides have acute toxicity and high bioaccumulation potential in the environment. Therefore, there is growing interest to develop methods to eliminate the toxic chlorine groups in aryl chlorides. Among the various detoxification techniques, the catalytic hydrodechlorination (HDC) is a preferred choice because it does not generate toxic compounds and the remaining hydrocarbons can be recycled.[2] To date, precious metals such as Pt,[3] Rh[4] and Pd,[5] and transition metals such as Ni,[6] Fe[7] and Co[8] are the most frequently used catalysts for HDC in either liquid- or gas-phase environments. Pd has exhibited superior performance than other metal catalysts in terms of activity and selectivity.[9] However, it suffers from deactivation due to coke deposition,[10] formation of surface metal halides,[11] or leaching of the active species.[12] In order to enhance the durability of Pd, a second metal is incorporated to modify its surface geometric arrangement and electronic properties. Several bimetallic catalysts such as Pd-Cu,[13] Pd-Ag,[14] Pd-Pt,[15] Pd-Ni,[16] and Pd-Fe[17] have been reported, with improved catalytic performance over their corresponding monometallic counterparts. Many reports have mentioned a beneficial effect of Au on Pd for a number of hydrogenation reactions, such as the hydrogenation of aromatic compounds,[18] the hydrogenation of dienes,[19] and the HDC of trichloroethene.[20] However, to the best of our knowledge, the utilization of SiO₂ supported Au-Pd bimetallic catalysts for the HDC of aryl chlorides has not been reported so far.[9, 21]

Several methods have been proposed to prepare uniform bimetallic nanoparticles. Wet impregnation is a conventional method that can prepare a variety of supported Au-Pd catalysts,[22, 23] but usually with large size and severe agglomeration of particles. Recently, Hutchings et al. reported a novel method to support Au-Pd nanocrystals on activated carbon via a sol-immobilization technique.[24] Nevertheless, the protecting agents (such as PVP) must be removed by high-temperature calcination before catalytic performance tests, which inevitably leads to agglomeration of the Au-Pd nanoparticles.[25] Our earlier work reported an *in-situ* method to anchor Au nanoparticles on the organic-inorganic hybrid silica with reducible functional groups (–SiCH₂CH₂CH₂NHCH₂OH).[26] In the present work, we explore this method to synthesize supported Au-Pd bimetallic catalysts. The Au-Pd bimetallic nanoparticles exhibited high mixture homogeneity of the two components and high dispersion on the support. The addition of Au significantly improved the dispersion of Pd, and the catalytic performance for HDC of chlorobenzene was greatly improved.

2. Experimental

2.1. Catalyst Synthesis

The organic–inorganic hybrid silica supported Au-Pd nanoparticles were prepared according to our previous work.[26] First, 4.7 mL of 3-aminopropyl-triethoxy-silane (APTES) was added into 150 mL of deionized water. Then, 2.0 mL of formaldehyde solution (37%) was added into the mixture and induced a rapid hydrolysis in APTES, indicated by a white precipitate that formed in less than 30 s. After stirring at room temperature for 2 h, the obtained solid was filtered and washed with an excess amount of deionized water. The solid was then dried in vacuum at 120 °C for 12 h, which yielded a solid white

powder.

Au-Pd bimetallic catalysts were prepared as follows. First, 1.0 g of SiO$_2$-org was impregnated with an aqueous solution of PdCl$_2$ and HAuCl$_4$, at various Pd/Au molar ratios, at 100 °C for 2 h under stirring. The mixture was filtered and washed with an excess amount of deionized water until no chlorine ions were detected in the filtrate. Following drying in vacuum at 120 °C for 12 h, Au-Pd/SiO$_2$ catalyst samples were obtained, with Pd/Au molar ratios of 0.2, 1.0, and 2.0. Supported monometallic Au and Pd NPs, employed as controls, were prepared in the same manner. The metal loadings of all five catalysts are shown in Table 1.

2.2. Catalyst Characterization

The gold and palladium contents in the Au-Pd/SiO$_2$ catalysts were analyzed by means of inductively coupled plasma–atomic emission spectroscopy (ICP-AES) after the sample was dissolved in aqua regia. X-ray diffraction (XRD) analysis was carried out on a PW3040/60 X' Pert PRO (PANalytical) diffractometer (Cu Kα X-ray source, operated at 40 kV and 50 mA). Transmission electron microscopy (TEM) images were recorded using a FEI Tecnai G2 Spirit microscope operated at 120 kV. Scanning transmission electron microscopy (STEM) images were recorded on a FEI Tecnai G2 F30 S-Twin microscope that was operated at 300 kV. An energy-dispersive X-ray (EDX) spectroscopic detecting unit was used to collect the EDX spectra for elemental analysis. The specimen was prepared by ultrasonically dispersing the solid powder into ethanol and drops of the suspension were deposited onto a clean carbon-enhanced copper grid and then dried in air. X-ray photoelectron spectroscopy (XPS) spectra were obtained with a VG ESCALAB 250 equipped with a monochromated Al–Kα radiation source (1486.6 eV) under a residual pressure of 10^{-9} Torr. The binding energy scale was referenced to C1s at 284.6 eV.

2.3. Catalyst Evaluation

In a typical reaction procedure, Au-Pd/SiO$_2$ (0.10 g) was added to a stirred ethanol solution of chlorobenzene (CB) (0.338 g), triethylamine (Et$_3$N) (0.455 g, 1.5 equivalence vs. the number of chlorine atoms) and 40 ml solvent in a 50 ml reactor equipped with a mechanical stirring system under mild conditions (25 °C, 1 atm H$_2$). The product yield was quantified by GC-FID (Shanghai Tianmei, GC7890 II equipped with an HP-5 column (30 m × 0.32 mm × 0.25 μm)) analysis using mesitylene as internal standard. The injection-port temperature was 250 °C, the detector temperature was 280 °C, and the oven temperature was held at 120 °C. Conversion of the CB was calculated based on the following equation:

$$\text{Conversion (\%)} = \frac{C_0 - C_t}{C_0} \times 100$$

where C_0 is the concentration of the CB before reaction (mg/L); C_t is the concentration of the CB after a certain reaction time (mg/L).

For the recyclability test, the Au-Pd/SiO$_2$ catalyst was separated after reaction from the reaction mixture by centrifugation. The filtrate was then thoroughly washed with water and ethanol, dried at 120 °C in vacuum, and then reused as catalyst for the next run.

3. Results and Discussion

3.1. Catalyst Characterization

3.1.1. TEM/STEM

TEM images of the Au/SiO$_2$, Pd/SiO$_2$, and bimetallic AuPd$_{1.0}$/SiO$_2$ catalysts are presented in Fig. 1. For all samples, the particles were uniformly dispersed on the SiO$_2$ support with sizes below 4 nm. Unfortunately, Au-Pd bimetallic nanoparticles cannot be determined or distinguished from the corresponding monometallic counterparts by TEM or HRTEM, since Au and Pd have the same crystal structure and similar lattice parameters.[21] In
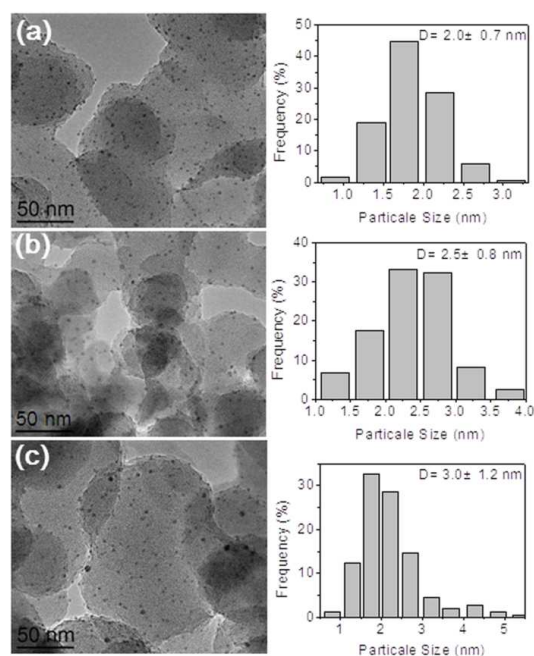
Fig. 1 Set of TEM images and corresponding size distribution from particles at the (a) Au/SiO$_2$, (b) Pd/SiO$_2$, and (c) AuPd$_{1.0}$/SiO$_2$ catalysts.
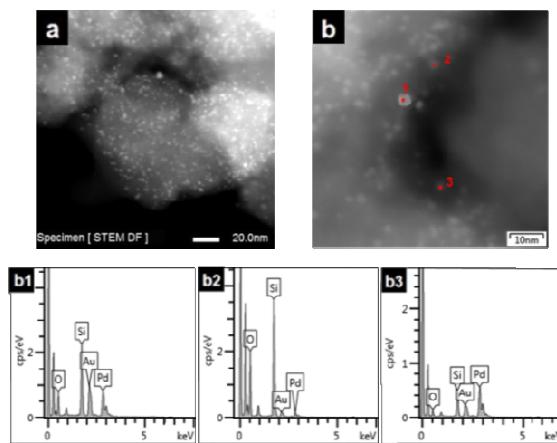
Fig. 2 HAADF-STEM images of as-synthesized (a) AuPd$_{1.0}$/SiO$_2$ sample and EDX point analysis spectra of the selected area 1 (b1), 2 (b2) and 3 (b3).

order to obtain the composition of the Au-Pd bimetallic nanoparticles, high-angle annular dark-field STEM (HAADF-STEM) and EDX were used to analyze the randomly selected NPs from the representative $AuPd_{1.0}$ bimetallic catalyst. As shown by the HAADF-STEM image, the Au-Pd bimetallic NPs immobilized by SiO_2 were in size of 3-4 nm (Fig. 2a), almost identical to that obtained from TEM. Both the signal of Au and

Pd were detected in all the bright spots randomly chosen (Fig. 2 b1, b2, and b3), indicative of a highly intimately mixed phase of Au-Pd had been formed in bimetallic nanoparticles rather than physical mixtures of pure Au and Pd particles.[24, 27] It should be noted that the electron beam for EDX measurements was < 0.8 nm in diameter, which is much smaller than the size of the Au-Pd NPs.

Table 1 XPS Pd 3d and Au 4f binding energies (eV) and surface atomic ratios of the catalysts.

Sample	Metal loading (wt.%)[a]	Peak position [eV]		Pd^{II} [%]	Atomicratio Pd/Au[b]
		$Au^0\,4f_{7/2}$	$Pd^0\,3d_{5/2}$		
Au/SiO_2	Au 1.0(1.1)	84.4	-	-	-
$AuPd_{0.2}/SiO_2$	Au 1.0 (1.2) Pd 0.11 (0.11)	84.2	334.1	6.8	0.14 (0.17)
$AuPd_{1.0}/SiO_2$	Au 1.0 (1.2) Pd 0.54 (0.56)	83.7	334.3	20.9	1.0 (0.86)
$AuPd_{2.0}/SiO_2$	Au 1.0 (0.94) Pd 1.08 (0.862)	84.3	334.6	32.1	1.85 (1.89)
Pd/SiO_2	Pd 0.5 (0.54)	-	335.0	72.3	-

[a] The theoretical metal loading of Au-Pd, and the datum in parentheses is the actual metal loading measured by ICP-AES. [b] The atomic ratio of Pd/Au

measured by XPS, and the datum in parentheses is theratio value measured by ICP-AES.

3.1.2. XRD

Fig. 3 shows the XRD patterns of the $AuPd_x/SiO_2$ samples. There were no obvious diffraction peaks resolved in the XRD patterns of the Au/SiO_2, Pd/SiO_2, and $AuPd_{0.2}/SiO_2$ except a broad diffraction peak that is attributed to the SiO_2 support. This can be explained by the fact that the lower loading of Au and Pd NPs were highly dispersed on the support and in small size below the detection limit of the X-ray beam.[28] As the Pd loading increased, a weak and broad diffraction peak ranging from 38° to 40° emerged, indicating the Pd atoms entered into the crystal lattice of Au, forming Pd-Au bimetallic NPs rather than a mixture of Pd and Au NPs.[25,29]
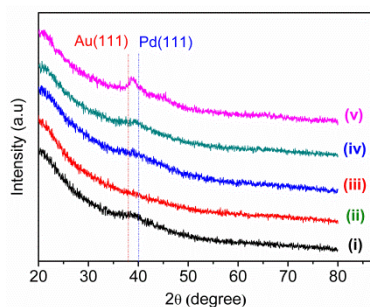
Fig. 3 XRD patterns for the catalysts (i) Au/SiO_2, (ii) Pd/SiO_2, (iii) $AuPd_{0.2}/SiO_2$,(iv) $AuPd_{1.0}/SiO_2$, and (v) $AuPd_{2.0}/SiO_2$.

3.1.3. UV−Vis Spectra

From the DR UV−vis spectrum (Fig. 4), the Au/SiO_2 sample exhibited a peak maximimum at 530 nm, which was attributed to the surface plasmon resonance (SPR) of the Au NPs.[30] However, this peak disappeared upon the addition of Pd. It has been shown that the incorporation of Pd to the crystal lattice of Au can change the band structure of Au, resulting in the absence of the SPR peak.[24, 31, 32]
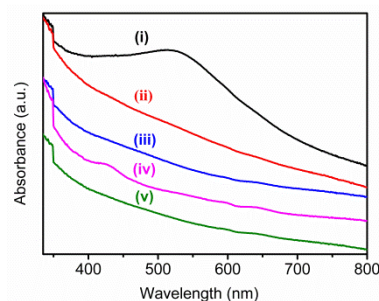
Fig. 4 UV−vis spectra for the catalysts (i) Au/SiO_2, (ii) $AuPd_{0.2}/SiO_2$, (iii) $AuPd_{1.0}/SiO_2$, (iv) $AuPd_{2.0}/SiO_2$, and (v) Pd/SiO_2.

3.1.4. XPS

To obtain further information about the structure and electronic properties of the bimetallic NPs, XPS characterization was performed for the three $AuPd_x/SiO_2$ catalysts. Fig. 5 and Table 1 show the fitted XPS spectra and the resulting data, respectively.

The XPS data showed that both the peaks ascribed to Au^0 4f and Pd^0 3d shifted to lower binding energy with respect to the monometallic Au/SiO_2 and Pd/SiO_2. Such an observation was reported previously and attributed to the modification of the electronic structure of Au by the incorporation of Pd atoms.[33] In the Pd 3d spectra, the peaks with the binding energies of 335.0 and 340.2 eV were attributed to the Pd^0 $3d_{5/2}$ and $3d_{3/2}$ in monometallic Pd/SiO_2. However, a negative shift of 0.9 eV was observed for the Pd^0 $3d_{5/2}$ and $3d_{3/2}$ peaks in the $AuPd_{0.2}/SiO_2$. Further increasing the Pd loading, the negative binding energy shift in the Pd^0 peaks showed a gradual decrease to 0.7 eV for $AuPd_{1.0}/SiO_2$ and 0.4 eV for $AuPd_{2.0}/SiO_2$. The large span of the binding energy (BE) shifts correspond to a strong interaction between Au and Pd.[34] The homogeneity of the Au-Pd bimetallic NPs appears to be dependent on the Pd content. While Pd was uniformly dispersed within Au at low Pd content, the

incorporated Pd would be isolated from Au and exist as islands when Pd was in excess.

In addition to Pd[0], the deconvolution of the Pd 3d XPS spectra of all the samples gave another two peaks ascribed to the Pd^{2+} 3d$_{5/2}$ and 3d$_{3/2}$. The formation of the Au-Pd bimetallic NPs significantly reduced the degree of Pd oxidation, as indicated by the decreased fraction of Pd^{2+} species. This phenomenon implies that the interaction between Au and Pd might result in the modification of the electronic structure of Pd, which facilitated the protection of Pd from oxidation.[35,36] The ratios of Pd/Au calculated from the XPS data demonstrate that there is no obvious surface enrichment of either Pd or Au, excluding the possibility for a core-shell structure.
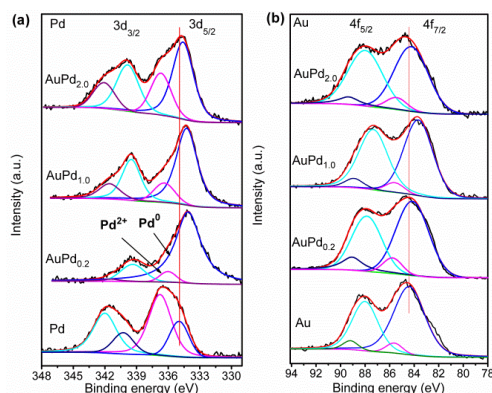
Fig. 5 XPS spectra of (a) Pd 3d and (b) Au 4f in the different catalysts.

3.2. HDC Reaction

It has been reported that the HCl generated during the HDC reaction could poison Pd and severely reduce the reaction rate.[37] Hence, in the present case, a base (Et$_3$N) was used to neutralize HCl. Since the aromatic ring resonance stability enough, benzene was produced selectively and none of the ring hydrogenated compounds were detected under the mildness condition. The Pd/SiO$_2$ showed a relatively low activity with the conversion of only 78.2% CB in 5 h, whereas the Au/SiO$_2$ was almost not active in the HDC reaction (Fig. 6a). However, the Au-Pd bimetallic NPs showed greatly enhanced activity compared with the Pd/SiO$_2$, suggesting a key role of Au in promoting HDC activity. The optimal AuPd$_{1.0}$/SiO$_2$ catalyst could complete the conversion of CB within 2 h. The promotion of the activity of Pd upon the addition of the inert Au could be explained by the dilution and electronic effects. In this case, the Pd was diluted and formed islands on the surface defects of Au, providing more active sites than pure Pd surface.[9,38] In addition, the modification of the electronic properties of Pd by Au could also contribute to the enhancement of the Pd activity. Except for the active sites on Pd, the bimetallic Pd-Au NPs could also provide Pd-Au interfacial sites as new active sites for the HDC reaction.[9] Furthermore, the inert Au atoms can adsorb the chlorine atoms[39] and weaken the C−Cl bond, facilitating the elimination of Cl and preventing Pd from poisoning.

Two mechanisms of the HDC reaction of aromatic chlorides have been proposed by Likholobov and co-workers.[40] If the HDC proceeds by a radical mechanism, the formed phenyl radicals either interact with the adsorbed hydrogen atoms to form benzene or recombine to form diphenyl.[38] Since the latter was not detected in the current work, it is presumed that the reaction proceeded as follows (Fig. 6b). Au induced the adsorption of CB and Pd served to activate H$_2$. The adsorbed H formed on the Pd surface reacted with the adsorbed CB to generate benzene and HCl. The base was used to neutralize the HCl and inhibit the poisoning of Pd.
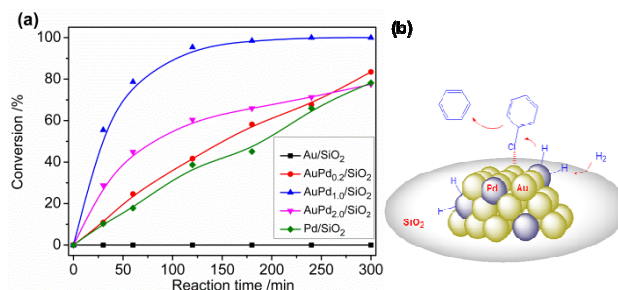
Fig. 6 Conversion for the HDC of CB with various catalysts (a) and proposed reaction mechanism of HDC reaction over AuPd$_x$/SiO$_2$ (b).

3.3. Effect of Base
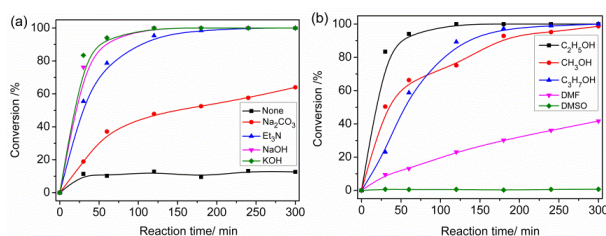
Fig. 7 The effect of different bases (a) and solvents (b) on the HDC of CB over AuPd$_{1.0}$/SiO$_2$.

The effect of the base in the HDC of CB was investigated over the most active AuPd$_{1.0}$/SiO$_2$ catalyst (Fig. 7a). The results indicated that the conversion of CB was significantly affected by the basicity of neutralizer. When no base was added, the conversion of CB reached 10% within 30 min but a rapid activity loss of the catalyst was observed in the following period. Once the neutralizer was added, the reaction equilibrium moved to the right and the reaction rate was accelerated. In this case, the HDC reaction rate decreased in the order of KOH ≈ NaOH > Et$_3$N > Na$_2$CO$_3$, consistent with the decreasing basicity of neutralizer. This confirms that a strong base was more effective to neutralize the HCl.[14] Although Na$_2$CO$_3$ and Et$_3$N have almost identical basicity, the reaction rate in Et$_3$N system was much higher than that in Na$_2$CO$_3$. This might be due to the fact that Et$_3$N possessed a better solubility in ethanol than Na$_2$CO$_3$.[41]

3.4. Effect of Solvent

Solvent effects on the HDC of CB were investigated over AuPd$_{1.0}$/SiO$_2$ using KOH as the base (Fig. 7b). The results showed that ethanol was the most preferable solvent for this reaction, followed by methanol, i-propanol, dimethylformamide (DMF), and dimethylsulfoxide (DMSO). Wang and co-workers reported that the increase in the polarity of solvent favored the transfer of chloride species from the catalyst surface to the reaction liquor.[42] The highest activity for the HDC of CB was obtained in methanol rather than *n*-hexane with weak polarity.

However, applying strong polarity solvents (i.e., DMF, DMSO) in the present case greatly reduced the catalytic activity. Especially when DMSO was used as the solvent, no desired products were produced. This is likely due to the high [5] coordination ability of these solvents, which might deactivate the active sites by interacting strongly with the metal center.[43] A desired result was obtained with the less polar protic solvents, such as ethanol, methanol, and i-propanol. Protic solvents have been reported to be hydrogen donors in many hydrogenation [10] reactions. Thus, hydrogen transfer processes in these solvents could benefit the hydrogenation involved in the HDC reaction, leading to the better catalytic performance.

3.5. Recycling Study

The leaching of active species is a significant problem that causes [15] deactivation of many heterogeneous catalysts.[12] In this case, after separation and appropriate pretreatment, the $AuPd_{1.0}/SiO_2$ could still achieve a conversion of CB of 83% in 1h in the fifth test (Fig. 8). This demonstrates that the bimetallic Au-Pd catalyst has good durability. The metal content of the catalysts was determined by [20] ICP after the fifth test. The result of Au(0.75wt.%)Pd(0.43wt.%)/SiO_2 implied only trace metal leaching during the recycling tests. This might be contributed by the efficient anchoring of the NPs by the amine groups in the SiO_2 support.

[25]
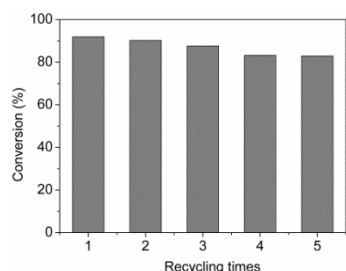
Fig. 8 Conversions of CB HDC over recycled $AuPd_{1.0}/SiO_2$ catalysts at $25°C$ within 1 h.

4. Conclusions

Highly dispersed Au-Pd NPs with small size have been prepared [30] through a facile *in-situ* reduction method. The results reveal that high homogeneity of the two components have been formed in all the bimetallic catalysts, and a pronounced composition-dependent catalytic activity of $AuPd_x/SiO_2$ in the HDC reaction was observed. Furthermore, the catalyst is easily recoverable and can [35] be reused several times without obvious leaching or loss of activity. The significantly improved catalytic performance of the bimetallic catalyst can be ascribed to the high dispersion and modified electronic properties of Pd. However, the intrinsic mechanism underlying these effects still requires further [40] investigation.

Notes and references

aState Key Laboratory of Fine Chemicals, School of Chemstry, Dalian University of Technology, Dalian 116024, China. Fax: +86-411-84986329; E-mail: wangxinkui@dlut.edu.cn.
[50] *b Laboratory of Advanced Materials and Catalytic Engineering, School of Chemstry, Dalian University of Technology, Dalian 116024, China*
c State Key Laboratory of Catalysis, Dalian Institute of Chemical Physics, Chinese Academy of Sciences, Dalian, 116023, China

1   T. Kawabata, I. Atake, Y. Ohishi, T. Shishido, Y. Tian, K. Takaki
[55]   and K. Takehira, Appl. Catal., B, 2006, 66, 151.
2   B. F. Hagh and D. T. Allen, Chem. Eng. Sci., 1990, 45, 2695.
3   S. Srinivas, P. S. Prasad and P. K. Rao, Catal. Lett., 1998, 50, 77.
4   M. Aresta, A. Dibenedetto, C. Fragale, P. Giannoccaro, C. Pastore, D. Zammiello and C. Ferragina, Chemosphere, 2008, 70, 1052.
[60] 5   T. Hara, K. Mori, M. Oshiba, T. Mizugaki, K. Ebitani and K. Kaneda, Green Chem., 2004, 6, 507.
6   N. Lingaiah, M. A. Uddin, A. Muto, T. Iwamoto, Y. Sakata and Y. Kusano, J. Mol. Catal. A: Chem., 2000, 161, 157.
7   I. Mishakov, V. Chesnokov, R. Buyanov and N. Pakhomov,
[65]   Kinet. Catal., 2001, 42, 543.
8   J. Cecilia, A. Infantes-Molina, E. Rodríguez-Castellón and A. Jiménez-López, J. Hazard. Mater., 2013, 260, 167.
9   Z. Wu, C. Sun, Y. Chai and M. Zhang, RSC Advan., 2011, 1, 1179.
10 E. Creyghton, M. Burgers, J. Jansen and H. Van Bekkum,
[70]   Appl. Catal., A, 1995, 128, 275.
11 C. Park, C. Menini, J. L. Valverde and M. A. Keane, J. Catal., 2002, 211, 451.
12 Y. Huang, S. Liu, Z. Lin, W. Li, X. Li and R. Cao, J. Catal., 2012, 292, 111.
[75] 13 S. Lambert, F. Ferauche, A. Brasseur, J.-P. Pirard and B. Heinrichs, Catal. Today, 2005, 100, 283.
14 H. Rong, S. Cai, Z. Niu and Y. Li, ACS Catal., 2013, 3, 1560.
15 M. Legawiec-Jarzyna, A. Śrebowata, W. Juszczyk and Z. Karpiński, Appl. Catal., A, 2004, 271, 61.
[80] 16 N. Seshu Babu, N. Lingaiah and P. Sai Prasad, Appl. Catal., B, 2012, 111, 309.
17 T. Zhou, Y. Li and T.-T. Lim, Sep. Purif. Technol, 2010, 76, 206.
18 Y. Xiang, Q. Meng, X. Li and J. Wang, Chem. Commun., 2010, 46, 5918.
[85] 19 N. E. Kolli, L. Delannoy and C. Louis, J. Catal., 2013, 297, 79.
20 K. N. Heck, M. O. Nutt, P. Alvarez and M. S. Wong, J. Catal. 2009, 267, 97.
21 X. Yuan, G. Sun, H. Asakura, T. Tanaka, X. Chen, Y. Yuan, G. Laurenczy, Y. Kou, P. J. Dyson and N. Yan, Chem. Commun., 2013,
[90]   19, 1227.
22 N. Dimitratos, J. A. Lopez-Sanchez, J. M. Anthonykutty, G. Brett, A. F. Carley, R. C. Tiruvalam, A. A. Herzing, C. J. Kiely, D. W. Knight and G. J. Hutchings, Phys. Chem. Chem. Phys., 2009, 11, 4952.
23 J. K. Edwards, N. Ntainjua, A. F. Carley, A. A. Herzing, C. J. Kiely
[95]   and G. J. Hutchings, Angew. Chem. Int. Ed., 2009, 48, 8512.
24 J. Pritchard, L. Kesavan, M. Piccinini, Q. He, R. Tiruvalam, N. Dimitratos, J. A. Lopez-Sanchez, A. F. Carley, J. K. Edwards and C. J. Kiely, Langmuir, 2010, 26, 16568.
25 X. Wei, X.-F. Yang, A.-Q. Wang, L. Li, X.-Y. Liu, T. Zhang, C.-Y.
[100]   Mou and J. Li, J. Phys. Chem. C, 2012, 116, 6222.
26 X. Tan, Z. Zhang, Z. Xiao, Q. Xu, C. Liang and X. Wang, Catal. lett., 2012, 142, 788.
27 X. Gu, Z.-H. Lu, H.-L. Jiang, T. Akita and Q. Xu, J. Am. Chem. Soc., 2011, 133, 11822.
[105] 28 B. Pawelec, A. M. Venezia, V. La Parola, S. Thomas and J. Fierro, Appl. Catal., A, 2005, 283, 165.
29 G. Zhang, Y. Wang, X. Wang, Y. Chen, Y. Zhou, Y. Tang, L. Lu, J. Bao and T. Lu, Appl. Catal., B, 2011, 102, 614.
30 S. Link, Z. L. Wang and M. El-Sayed, J. Phys. Chem. B, 1999, 103,
[110]   3529.
31 S. Deki, K. Akamatsu, Y. Hatakenaka, M. Mizuhata and A. Kajinami, Nanostruct. Mater., 1999, 11, 59.
32 J. A. Lopez-Sanchez, N. Dimitratos, P. Miedziak, E. Ntainjua, J. K. Edwards, D. Morgan, A. F. Carley, R. Tiruvalam, C. J. Kiely and G.
[115]   J. Hutchings, Phys. Chem. Chem. Phys, 2008, 10, 1921.

33   J. Long, H. Liu, S. Wu, S. Liao and Y. Li, ACS Catal., 2013, 3, 647.
34   R. Wang, Z. Wu, C. Chen, Z. Qin, H. Zhu, G. Wang, H. Wang, C. Wu, W. Dong and W. Fan, Chem. Commun., 2013, 49, 8250.
35   X. Yang, D. Chen, S. Liao, H. Song, Y. Li, Z. Fu and Y. Su, J. Catal., 2012, 291, 36.
36   K. Qian and W. Huang, Catal. Today, 2011, 164, 320.
37   G. Yuan and M. A. Keane, Appl. Catal., B, 2004, 52, 301.
38   M. O. Nutt, K. N. Heck, P. Alvarez and M. S. Wong, Appl. Catal., B, 2006, 69, 115.
39   G. N. Kastanas and B. E. Koel, Appl. Surf. Sci., 1993, 64, 235.
40   V. Yakovlev, V. Terskikh, V. Simagina and V. Likholobov, J. Mol. Catal. A: Chem., 2000, 153, 231.
41   C. Xia, Y. Liu, J. Xu, J. Yu, W. Qin and X. Liang, Catal. Commun., 2009, 10, 456.
42   Z. Jin, C. Yu, X. Wang, Y. Wan, D. Li and G. Lu, J. Hazard. Mater., 2011, 186, 1726.
43   R. Abazari, F. Heshmatpour and S. Balalaie, ACS Catal., 2012, 3, 139.

RSC Advances Accepted Manuscript